# Preparation of activated carbon as support of nickel catalyst for Guerbet reaction

**Krittanun Deekamwong[1], Supunnee Junpirom[2] and Jatuporn Wittayakun[1]***

[1] School of Chemistry, Institute of Science, Suranaree University of Technology, Nakhon Ratchasima, 30000 Thailand
[2] School of Chemical Engineering, Institute of Engineering, Suranaree University of Technology, Nakhon Ratchasima, 30000 Thailand

*\*Corresponding author: jatuporn@sut.ac.th*

## Abstract

This work aims to prepare activated carbon from charcoal from the wood of *Muntingia calabura Linn*. and employ as support for nickel catalyst. The charcoal was obtained from an Iwasaki kiln and activated by $CO_2$. Then, the surface of activated carbon was modified by air zero to create acid functional groups. The polyaromatic-like structure and functional groups of the activated carbon were characterized by Fourier transform infrared spectroscopy (FTIR) and elemental analysis. The thermal stability was carried out by thermogravimetric analysis (TGA). The surface areas of the samples were determined by Brunauer–Emmett–Teller (BET) from $N_2$ adsorption-desorption analysis. The activated carbon after modification had higher acid functional groups than the parent charcoal. The BET surface area decreased after modification, but the thermal stability did not change after $CO_2$ treatment. After impregnated with nickel precursor, the phases of the catalyst were analyzed by X-ray diffraction (XRD). Nickel nanoparticles were produced on activated carbon. The catalytic screening of Guerbet reaction to produce *n*-butanol from ethanol conversion was performed under autogeneous pressure at 240 °C for 6 h. The nickel supported on activated carbon showed higher ethanol conversion than the unsupported nickel nanoparticles.

**Keywords**: *Muntingia calabura Linn*.; activated carbon; nickel nanoparticles, catalyst, guerbet reaction

## Introduction

It is possible that *n*-butanol could become a part of biofuels, especially for transportation according to its high heating value, high flash point, low oxygen content and miscibility with diesel and gasoline. Currently, a commercial method to produce *n*-butanol is fermentation from food. However, the production capacity, competition with food and toxicity from bacteria are concerned (Kaminski et al., 2011). The research process is shifted to a chemical reaction of ethanol from biomass in the presence of a heterogeneous catalyst. Riittonen et al. (2012) have studied a one-pot liquid-phase reaction. They have concluded that Ni metallic form supported on $Al_2O_3$ (Ni/$Al_2O_3$) shows a better catalytic activity than the supported Pt, Pd, Ag and Co. Then, Zhang et al. (2013) have revealed a simple and environmentally friendly method to produce *n*-butanol by Guerbet process (see equation below) with Co metal powder in a hydrothermal batch reactor at 240 °C and autogenous pressure; a good yield and high selectivity are obtained. Although a good reaction pathway of *n*-butanol is developed (Zhang et al., 2013), the catalyst is still expensive. This problem could be solved by dispersing the metal active phase on porous materials.

Guerbet process:

$$2CH_3CH_2OH \rightarrow CH_3CH_2CH_2CH_2OH + H_2O$$

Activated carbon is a porous material which is widely used as a support for nickel catalyst (Fidalgo et al., 2010; Rios et al., 2003; Vasu et al., 2008; Wojcieszak et al., 2006; Yao et al., 2008). Thus, nickel on activated carbon could give high nickel active sites. This property could help to upgrade the catalytic activity on the Guerbet process.

Activated carbon is widely used as catalyst support because it has a high surface area, acid/base resistivity and low cost of production. Typically, the activated carbon is prepared from a lignocellulosic material by pyrolysis and physical/chemical treatment. The layers of the polyaromatic-like molecules contain acid/base functional groups. Junpirom et al. (2007) have investigated the surface modification by chemical and physical treatment. The physical treatment by air zero is a suitable and environmentally friendly method to increase the acid sites on the activated carbon surface. Those acid functional groups are adsorption sites for cation (Azzi Rios et al., 2003; Vasu et al., 2008). Then, the cations could be reduced to form nanoparticles on activated carbon.

The goal in this work is to prepare activated carbon for the application as catalyst support. First, the wood of *Muntingia calabura Linn.*, a local plant from Nakhon Ratchasima province, Thailand, was pyrolyzed in an Iwasaki kiln to produce charcoal. Then, the charcoal was activated by carbon dioxide ($CO_2$) in a horizontal tube furnace. Finally, the activated carbon is used as a support for nickel catalyst for the synthesis of *n*-butanol from ethanol via the Guerbet process in a batch reactor under autogenous pressure at 240 °C.

## Experimental

### Preparation of charcoal in an Iwazaki kiln

The wood of *Muntingia calabura Linn.* with diameter of about 5-10 cm was collected from a local field near the university. It was cut to the length of about 80 cm and dried in air under sunlight for 30 days. The pyrolysis of *Muntingia calabura Linn.* wood was carried out in an Iwazaki kiln (Figure 1) at Energy Ashram, Appropriate Technology Association in Pakchong District, Nakhon Ratchasima. The furnace was built with a 200-litre oil tank connected with an asbestos tube and steel condenser. The optimum temperature and airflow were controlled by adjusting a gap in the front of the furnace. After about 10 h, the gap was closed and the furnace was cooled down to ambient temperature. The obtained charcoal was collected.



**Figure 1.** (Left) The actual Iwazaki kiln (Right) drawing to represent the parts.

### Preparation of activated carbon by $CO_2$ physical treatment

The charcoal of *Muntingia calabura Linn.* was activated by CO2 physical treatment in the horizontal tube furnace (Carbolite, UK) with a length of 122.2 cm and internal diameter of 3.8 cm (Junpirom et al., 2007). In each preparation, about 2 g of charcoal was crushed and sieved to average particle sizes between 2.1 mm – 0.714 µm, loaded in two ceramic boats and placed at the center of the furnace. It was heated from room temperature to 800 °C with a heating rate of 20 °C/min under $N_2$ flow (100 mL/min) followed by $CO_2$ flow (100 mL/min, Linde Gas, 99.95%) for 1 h. Finally, the furnace was turned off and cooled to the ambient temperature under $N_2$ flow. The obtained sample was named "AC".

### Modification of activated carbon surface by air zero physical treatment

The surface of activated carbon was modified by physical treatment in the horizontal tube furnace (Junpirom et al., 2007). In each preparation, about 2 g of activated carbon was crushed and sieved to average particle sizes between 2.1 mm – 0.714 µm, loaded in two ceramic boats and placed at the center of the furnace. It was heated from room temperature to 250 °C with a heating rate of 20 °C/min under N2 flow (100 mL/min) followed by air zero (100 mL/min, 21% $O_2$ in N2 balance) flow for 24 h. Finally, the furnace was turned off and cooled to the ambient temperature under $N_2$ flow. The obtained sample was named "Mod AC".

### Characterization of activated carbon and modified activated carbon

Functional groups of samples were determined by Fourier transform infrared spectroscopy (FTIR, Perkin Elmer, Spectrum GX). $N_2$ adsorption-desorption isotherm was obtained from a Micromeritics ASAP 2010. The surface area was calculated by the Brunauer–Emmett–Teller (BET) method. Thermal stability of the material was investigated by thermogravimetric and differential

Wittayakun et al.

*J. Sci. Agri. Technol. (2020) Vol. 1 (1): 33-39*

thermogravimetric analysis (TGA-DTA, TA Instrument/ SDT2960) under $N_2$ at the flow rate of 100 mL/min. The sample was heated from 40 to 900 °C at a heating rate 20 °C /min". The chemical composition was determined by CHNO elemental analysis (Leco, TruSpec Micro CHNO).

**Synthesis of nickel nanoparticle**

Nickel nanoparticles were synthesized by a method modified from Zhang et al. (2004) and Motuzas et al. (2014). A mixture with $OH^-$:$Ni^{2+}$ at the molar ratio of 4:1 was prepared by dissolving from 0.3553 g of nickel acetate tetrahydrate (98+%, Strem chemicals) and 2.2373 g of sodium hydroxide (technical grade, Carlo Erba) in 60 mL of ethylene glycol (technical grade, Carlo Erba). The resulting solution was transferred into a 100 mL microwave vessel, closed and heated via microwave irradiation in a Microwave MARs 6-One Touch in which the temperature is monitored by IR sensor with adjustable power output (300 W). The solution was heated with the rate of 5 °C/min to 180 °C and held at the final temperature for 15 min. After cooling to room temperature, the precipitate was filtered, washed with ethanol and dried at 160 °C overnight. The obtained sample was named "Nickel nanoparticle."

**Preparation of nickel supported on modified activated carbon by precipitation (Ni/Mod AC)**

One gram of modified activated carbon was dispersed in a 0.3553 g of nickel acetate tetrahydrate in 30 mL of ethylene glycol to allow nickel to adsorb on the surface for 12 h. Then, 2.2373 g of sodium hydroxide in 30 mL of ethylene glycol producing the $OH^-$:$Ni^{2+}$ at the molar ratio of 4:1 was added. The 10% w/w of $Ni^{2+}$ was expected. The resulting solution with the total volume of 60 mL was transferred into a 100 mL microwave vessel, closed and heated via a Microwave MARs 6-One Touch. The solution was heated with the rate of 5 °C/min to 180 °C and held at the final temperature for 15 min. After cooling to room temperature, the precipitate was filtered, washed with ethanol and dried at 160 °C. The obtained sample was named "Ni/Mod AC."

**Characterization of nickel nanoparticle and Ni/Mod AC**

Nickel nanoparticle and Ni/Mod AC was characterized by X-ray diffraction (XRD, Bruker D8 Advance), generating Cu-K$_\alpha$ radiation operating at a voltage of 40 kV and current of 40 mA. The crystalline size (D) was calculated by using the Scherrer's equation (Equation 1)

$$D = \frac{0.89\lambda}{\beta\cos\theta} \qquad (1)$$

where $\lambda$ is wavelength (1.5418 Å), $\beta$ is full width at half maximum (FWHM) of the peak and $\theta$ is the Bragg's angle of the XRD peak from the main diffraction peak. Functional group was analyzed by FTIR.

**Catalytic performance on hydrothermal synthesis of *n*-butanol from ethanol**

Catalytic reaction was done in a 450 mL of Parr 5500 compact reactor with the following procedure. The starting reagent solution containing 150 mL of ethanol (absolute, Carlo Erba), 4.2 g of $NaHCO_3$, 70 mL of water and 0.4 g of catalyst was added into the autoclave, sealed, placed in a furnace and heated to 240 °C for 6 h. The final autogenous pressure in the autoclave was around 55 bars as measured by a digital pressure gauge. After each test, the autoclave was quenched to room temperature by water-cooling.

Products were analyzed by a gas chromatograph equipped with flame ionization detector (GC-FID, Agilent G1530A) equipped DB-wax (polyethylene glycol) column. The 0.5 mL of sample and 0.1 mL of *n*-heptanol as an internal standard were diluted in 25 mL of water. The sample (0.1 μL) was injected with a 50:1 split mode. The injection and FID detector temperature were 180 °C and 100 °C, respectively. The temperature was programmed from 100 °C, ramp to 120 °C at 4 °C/min and then to 180 °C at 30 °C/min for 1 min.

The concentration of ethanol was determined from a standard curve produced by the ratio of peak height of ethanol and *n*-heptanol with various %v/v of ethanol. Then the conversion of ethanol was calculated by Equation 2 (Riittonen et al., 2015):

$$\text{Conversion of ethanol } (\%) = \left(\frac{C_0 - C_i}{C_0}\right) \times 100 \qquad (2)$$

where $C_0$ is the initial concentration of ethanol and $C_i$ is measured concentration of ethanol after catalytic reaction. The *n*-butanol selectivity was estimated from the ratio of the peak height of *n*-butanol and *n*-heptanol.

## Results and discussion

**Characterization of charcoal, activated carbon and modified activated carbon**

The FTIR spectra of the charcoal, AC and Mod AC and peaks assignment are shown in Figure2. From the charcoal sample, the bands corresponding to C–C aromatic carbon of polyaromatic-like structure and O–H bond were observed. After activation, the band corresponding to carbonyl

groups was observed and the C–C bond was retained (Hesas et al., 2013). Then, the O-H groups were displayed together with carbonyl groups in Mod AC (Hesas et al., 2013). Moreover, all samples showed C=N bond (Aboud et al., 2015). Therefore, the C–OH was transformed to C=O after activation and then converted to COOH after surface modification regarding to the presence of both C=O and C–OH functional groups.
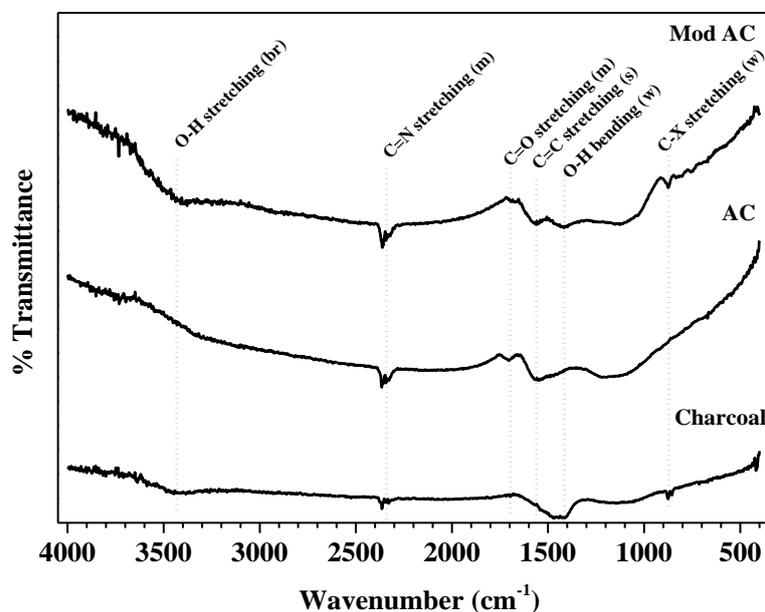


**Figure 2.** FTIR spectra of charcoal, AC and Mod AC; Intensity: br=broad, w=weak, m=medium and s=strong.

The elemental compositions of the charcoal, AC and Mod AC are shown in Table 1. The major component is carbon, followed by oxygen and trace of hydrogen and nitrogen. The carbon to oxygen (C/O) ratio implies the high amount of acid site. After activation and modification, the oxygen content increased indicating that the approximated acid sites were increased (Ngernyen et al., 2005).

**Table 1.** Elemental composition of charcoal, AC and Mod AC.

|         | C (%)  | H (%) | N (%) | O (%)  | C/O   |
|---------|--------|-------|-------|--------|-------|
| Charcoal | 83.185 | 2.929 | 0.792 | 6.294  | 13.22 |
| AC      | 82.284 | 1.531 | 1.180 | 10.680 | 7.705 |
| Mod AC  | 74.790 | 2.492 | 0.737 | 10.090 | 7.412 |

The TGA thermogrgams and % weight derivatives of AC and Mod AC are shown in Figure 3. The first weight loss at below 100 °C corresponded to removal of physisorbed water. The second weight loss between 100 – 700 °C referred to the decomposition of the surface functional group. The last weight loss at the temperature about 700 °C corresponded to the decomposition of activated carbon (Peng et al., 2014). The gradual weight loss probably attributed to the decomposition of surface functional groups. According to the weight change, the AC and Mod AC were thermally stable up to 400 °C and 550 °C, respectively. Thus, both samples were suitable as catalyst supports for a reaction condition below those temperatures.

$N_2$ adsorption-desorption isotherms of AC and Mod AC are shown in Figure 4  The adsorption at $P/P_0 < 0.1$ corresponded to monolayer adsorption (Hesas et al., 2013). The BET surface area of the AC was 412 $m^2.g^{-1}$. After modification, Mod AC had a lower volume adsorbed ($V_a$) and the BET surface area was 170 $m^2.g^{-1}$. The modification could cause the collapse of pores. It was also possible that the presence of functional groups, such as hydroxyl and carboxyl blocked $N_2$ to enter the pore (Ngernyen et al., 2005).

*Wittayakun et al.*

*J. Sci. Agri. Technol. (2020) Vol. 1 (1): 33-39*
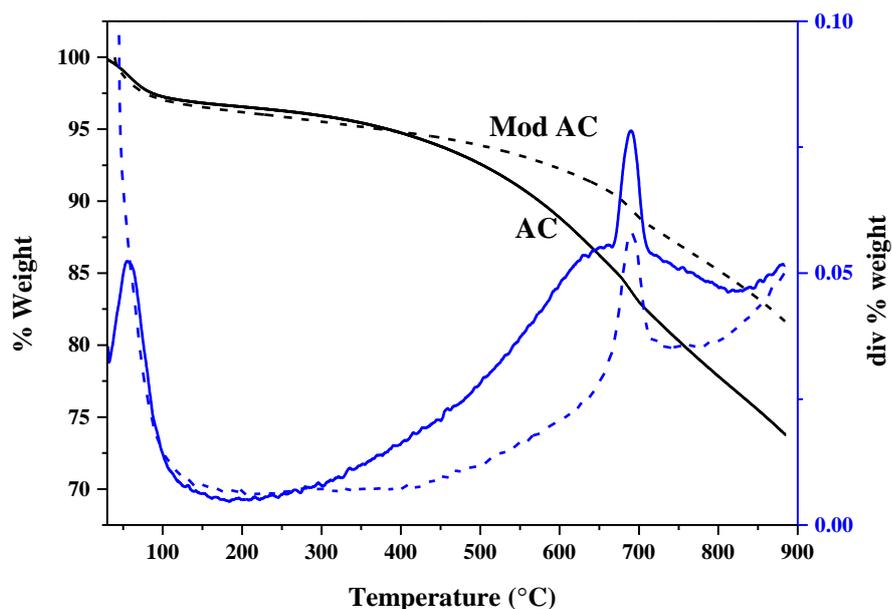
**Figure 3.** TGA Thermograms and % weight derivatives of AC (solid line) and Mod AC (dashed line).
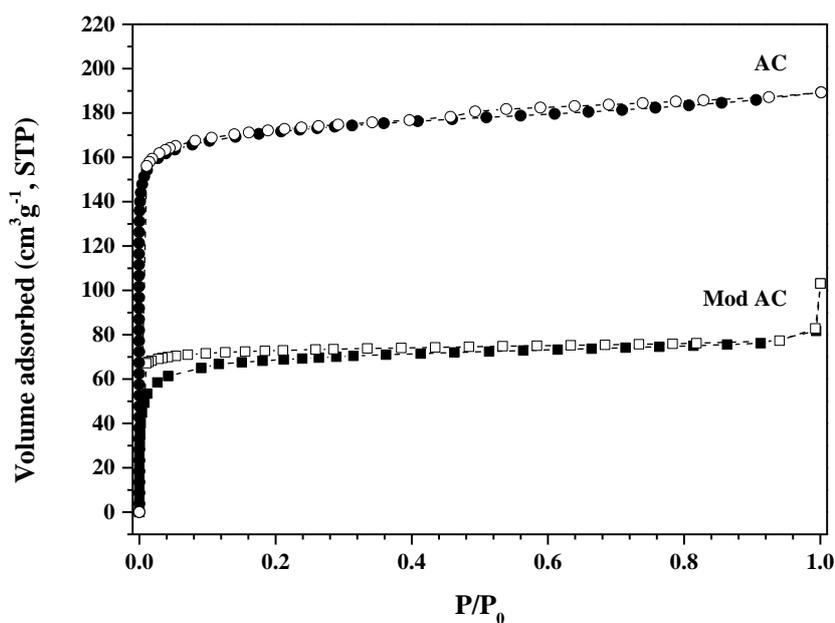


**Figure 4.** N2 adsorption-desorption isotherms of AC and Mod AC; adsorption (filled) and desorption (empty).

The XRD pattern of nickel nanoparticles is shown in Figure 5. The main diffraction peaks at 44.4, 51.8 and 76.2 degree were assigned to (100), (200) and (220) planes of metallic nickel form, respectively (Zhang et al., 2004). The sample did not show the peaks at 32.9, 38.5 and 51.7 degree corresponding to $Ni(OH)_2$ as intermediate phase and the peaks at 37.2, 43.3 and 62.9 degree corresponding to NiO (Motuzas et al., 2014; Dharmaraj et al., 2006). Nickel nanoparticles were synthesized successfully at 180 °C in 15 min. Thus, the crystalline size

calculated by Scherrer's equation was about 32 nm with 0.46 degree of FWHM. The method to synthesize nickel nanoparticle was improved by using a shorter time and lower temperature than that of the original method (Motuzas et al., 2014; Zhang et al., 2004).

The XRD pattern of nickel phase on modified activated carbon is shown in Figure 5. Nickel XRD pattern was similar to nickel nanoparticle. The crystalline size was about 50 nm by Scherrer's equation with 0.30 degree of FWHM.
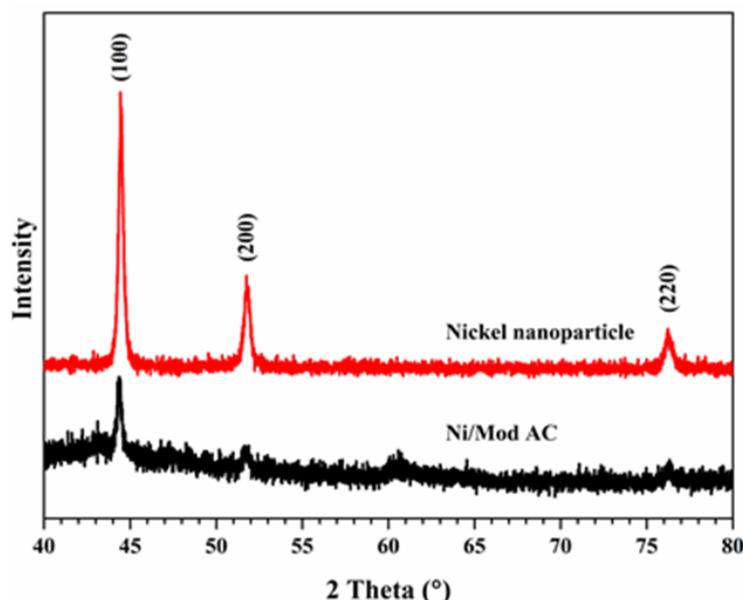
**Figure 5.** XRD patterns of nickel nanoparticles and Ni/Mod AC.

**Catalyst screening on Guerbet reaction**

Before catalytic testing, a blank test was carried out with the absence of a catalyst. The ethanol conversion was obtained (see Table 2). The NaHCO$_3$ in the solution could serve as a base catalyst to convert ethanol to acetaldehyde, butyraldehyde, crotonaldehyde, crotylalcohol, 2-butanol and *n*-butanol (Ndou et al., 2003).

By using 1 g of nickel nanoparticle catalyst, the ethanol conversion was more than two-fold higher than the blank test. Therefore, the nickel catalyst could be a hydrogen borrowing for dehydrogenation and hydrogenation. Both reactions produced two molecules of aldehyde (intermediate), butanal (intermediate) and butanol (Riittonen et al., 2012; Zhang et al., 2013). The ethanol conversion of Mod AC slightly increased compared to the blank test. However, there was no evidence to confirm the connection of these phenomena to the role of the bare supports.

The catalytic testing of nickel impregnated on Mod AC was carried out to see effect of metal dispersion. The supported catalyst showed a higher ethanol conversion than the nanoparticles. The role of support material on nickel catalyst resulted to improve catalytic conversion. The approximated *n*-butanol selectivity was the highest from nickel nanoparticle. However, the selectivity from Ni-Mod AC was higher than that from the parent support because of the presence of nickel nanoparticles. The lower selectivity might imply that the side reactions happened by the imbalance of acidic and basic catalysts of support and NaHCO$_3$ (Jordison et al., 2015).

**Table 2.** Ethanol conversion (%) and peak area of *n*-butanol fom the catalyst screening determined from GC-FID technique.

| Catalyst | Ethanol conversion (%) | | Peak area of *n*-butanol |
|---|---|---|---|
| | | Per mmole of Ni | |
| None | 6.1 | - | 0.071 |
| Nickel nanoparticle | 15.9 | 2.3 | 0.50 |
| Mod AC | 8.7 | - | 0.098 |
| Ni/Mod AC | 19.2 | 28.2 | 0.103 |

## Conclusions

Activated carbon was prepared from charcoal of *Muntingia calabura Linn.* wood by $CO_2$ physical treatment. Regarding FTIR and CHNO analysis, oxygen-containing functional groups referred to acid sites increased after activation and modification. Both AC and Mod AC showed high thermal stability. However, the surface area of modified activated carbon decreased because of pore-blocking by the presence of the functional group. Then, nickel catalyst (Ni/Mod AC) was prepared by dispersion of nickel nanoparticles on the Mod AC. The activity of *n*-butanol synthesis from ethanol conversion via Guerbet process was lower than that from other works. However, the multifunctional active site containing metal and acid/base is promising to improve the catalytic reaction.

## Acknowledgement

## References

Aboud, M.F.A., ALOthman, Z.A., Habila, M.A., Zlotea, C., Latroche, M. and Cuevas, F. 2015. Hydrogen storage in pristine and d10-block metal-anchored activated carbon made from local wastes. Energies. 8: 3578 – 3590.

Azzi Rios, R.R.V., Alves, D.E., Dalmázio, I., Bento, S.F.V., Donnici, C.L. and Lago, R.M. 2003. Tailoring Activated Carbon by Surface Chemical Modification with O, S, and N Containing Molecules. Materials Research. 6(2): 129 – 135.

Dharmaraj, N., Prabu, P., Nagarajan, S., Kim, C.H., Park, J.H. and Kim, H.Y. 2006. Synthesis of nickel oxide nanoparticles using nickel acetate and poly(vinyl acetate) precursor. Materials Science and Engineering: B. 128(1-3): 111 – 114.

Fidalgo, B., Zubizarreta, L., Bermúdez, J.M., Arenillas, A. and Menéndez, J.A. 2010. Synthesis of carbon-supported nickel catalysts for the dry reforming of CH4. Fuel Processing Technology. 91: 765 – 769.

Hesas, R.H., Arami-Niya, A., Daud, W.M.A.W. and Sahu, J.N. 2013. Preparation and characterization of activated carbon from apple waste by microwave-assisted phosphoric acid activation: application in methylene blue adsorption. BioResources. 8(2): 2950 – 2966.

Jordison, T.L., Lira, C.T. and Miller D.J. 2015. Condensed-phase ethanol conversion to higher alcohols. Industrial & Engineering Chemistry Research. 45: 10991 – 11000.

Junpirom, S., Tangsathitkulchai, C. and Tangsathitkulchai, M. 2007. Preparation of activated carbons from longan seed by physical and chemical methods (in Thai). Suranaree Journal of Science and Technology. 14(1): 63 – 76.

Kamiński, W., Tomczak, E. and Górak, A. 2011. Biobutanol - production and purification methods. Ecological Chemistry and Engineering S. 18: 31 – 37.

Motuzas, J., Drobek, M., Diniz da Costa, J.C. and Julbe, A. 2014. Novel microwave assisted approach to large scale nickel nanoparticle fabrication. Chemical Engineering Journal. 240: 155 – 160.

Ndou, A.S., Plint, N. and Coville, N.J. 2003. Dimerisation of ethanol to butanol over solid-base catalysts. Applied Catalysis A: General. 251: 337 – 345.

Ngernyen, Y., Tangsathitkulchai, C. and Tangsathitkulchai, M. 2005. The modification of acidic surface functionality of wood-based activated carbon. Suranaree Journal of Science and Technology.

Peng, G., Steib, M., Gramm, F., Ludwig, C. and Vogel, F. 2014. Synthesis factors affecting the catalytic performance and stability of Ru/C catalysts for supercritical water gasification. Catalysis Science & Technology. 4(9): 3329 – 3339.

Riittonen, T., Eränen, K., Mäki-Arvela, P., Shchukarev, A., Rautio, A.-R., Kordas, K., Kumar, N., Salmi, T. and Mikkola, J. 2015. Continuous liquid-phase valorization of bio-ethanol towards bio-butanol over metal modified alumina. Renewable Energy. 74: 369 – 378.

Riittonen, T., Toukoniitty, E., Madnani, D.K., Leino, A.-R., Kordas, K., Szabo, M., Sapi, A., Arve, K., Wärnå, J. and Mikkola, J.-P. 2012. One-pot liquid-phase catalytic conversion of ethanol to 1-butanol over aluminium oxide - the effect of the active metal on the selectivity. Catalysts. 2: 68 – 84.

Rios, R.R.A., Alves, D.E., Fernando, D.S., Bento, V., Donnici, L. and Lago, R.M. 2003. Tailoring Activated Carbon by Surface Chemical Modification with O, S, and N Containing Molecules. Material research. 6: 129 – 135.

Vasu, A.E. 2008. Surface Modification of Activated Carbon for Enhancement of Nickel(II) Adsorption. E-Journal of Chemistry. 5(4): 814 – 819.

Wojcieszak, R., Zieliński, M. and Bettahar, M.M. 2006. Study of nickel nanoparticles supported on activated carbon prepared by aqueous hydrazine reduction. Journal of Colloid Interface Science. 299(1): 238 – 248.

Yao, S., Yang, C., Tan, Y. and Han, Y. 2008. Deactivation and regeneration of an activated carbon-supported nickel catalyst for methanol carbonylation in the vapor phase. Catalysis Communications. 9(11–12): 2107 – 2111.

Zhang, F., Chen, Y., Zhao, J. and Li, H. 2004. Preparation of Nanosized Nickel Particles by Hydrothermal Method. Chemistry Letters. 33(2): 146 – 147.

Zhang, X., Liu, Z., Xu, X., Yue, H., Tian, G. and Feng, S. 2013. Hydrothermal synthesis of 1-butanol from ethanol catalyzed with commercial cobalt powder. ACS Sustainable Chemistry & Engineering. 1: 1493 – 1497.